The Incipit of Complexity in Self-Coupled Lasers

(from Deterministic Behaviour to Periodic Oscillations and to Chaos)

Silvano Donati and Valerio Annovazzi-Lodi
DIII – Department Industrial Engineering and Informatics
University of Pavia
v. Ferrata 1, 27100 Pavia, Italy
silvano.donati@ieee.org

***Abstract*— At the simplest level of implementation for an optical system, chaos and complexity are generated by the self-coupled laser configuration, when the field back-reflected from a remote target is allowed to re-enter in the laser cavity. The delay of the go-and-return path is the parameter governing complexity, and together with the second-order cavity resonance and coupling of gain to amplitude and phase, gives rise to a number of characteristic phenomena at increasing coupling, such as perturbed deterministic behavior, onset of period-one and period-two bifurcations, and finally route to chaos. We present detailed results of the regimes found in semiconductor laser subjected to a minute (a few percent) back-reflection, as a function of strenght of coupling K, propagation delay, and alfa-factor (or linewidth broadening). The portrait of regimes in the K-ϕ plane, where $\phi=2ks$ is the phase of the field returning from target distance s and $k=2\pi/\lambda$ is the wavevector, starts with unperturbed and period-1 bands to proceed, as distance s is increased, to zones of periodic regime sandwiched with increasing chaos bands, up to the point that all the K-ϕ space is filled with chaos. Using the new results, we will revisit the Tchak and Chaprivly (T-C) diagram of self-coupling, that is commonly used to diagnose disturbance effects in laser diodes intended for optical fiber communications. We show that the T-C diagram unveils intricated overlap of regimes. We then conclude with a focus on the several applications of the high level dynamics to measurement of optical paths, cryptography for communication of sensible data, and to high speed random number generation for computer applications.**

Keywords—coupled systems; optical chaos; self-mixing; high-level dynamics; laser diodes.

I. INTRODUCTION

Recently, the regime of coupling in laser sources has attracted considerable interest, and much work has been aimed to explain the new phenomena of complex dynamics and chaos as well to develop applications in communications and instrumentation. About configurations of coupling, *mutual coupling* occurs when two lasers exchange some of their power by injection into each other's cavity, and *self-coupling* when a single laser shines light onto an external reflector or diffuser and light backscattered from the target is allowed to re-enter the laser cavity, see Fig.1.

As described in a recent review paper [1], at a low level of interaction (say 10^{-8} to 10^{-3} for the ratio of exchanged power to in-cavity power), coupling generates amplitude (AM) and frequency (FM) modulations whose modulation indexes carry information on the coupling's amplitude and phase.

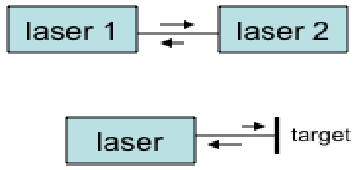

Fig 1 Schematic of coupled lasers. Top: mutual coupling (can be symmetrical or asymmetrical); bottom: self-coupling.

In particular, in *self-coupling* the phase is the optical phase-shift suffered on propagation to the target and back, a feature exploited in the application known as self-mixing interferometer, while dependence on amplitude is exploited in coherent detection of weak optical echoes [1].

At a high level of coupling (say from 10^{-3} to a few 10^{-1}), the laser oscillation is strongly perturbed and unveils new phenomena characteristic of complex-system dynamics, that is: bifurcations, period-one and multi-periodic amplitude oscillations, linewidth narrowing and broadening, and chaos [2-4]. Probably the most interesting application pursued in recent years internationally is chaos cryptography [4,5], a new technology exploiting the synchronization properties of matched chaos-generating systems. Remarkably, several versions of IPCs (Integrated Photonic Circuit), integrating in a single chip all the functions for a chaos-based system, like laser diode, phase modulator, waveguide and end-reflector have been developed within a single chip [6,7] which opens up the way for demonstrators and field trials of chaos cryptography.

Other applications of chaos or multi-period generation by coupled laser diodes start to appear, for example: random number generation [8], chaos-modulated rangefinders [9], and high-frequency tone generation by period-1 systems for radio-over-fiber applications [10,11].

In principle, we can develop all said applications either by mutual-coupling or self-coupling (also called DOF, delayed optical feedback). Of course, the latter has the practical advantage of minimum part count, requiring just a laser and a reflector, in lieu of two (usually tightly matched and frequency tunable) lasers, and is more easily amenable to integration.

To develop an IPC and incorporate also reflector and propagation, a short cavity length L. is also desirabl.e

Generally it is assumed [2,3,12,13] that a short (external) cavity is when the distance to the remote reflector, L, is small with respect to $L_{fr}=c/2f_r$, f_r being the relaxation frequency of the solitary laser. Several researchers (Schunk and Petermann [14], Mork et al. [13], Jones et al. [15]) have studied the regions of stability and coherence collapse at the boarderline of short cavity. At moderate feedback [1-3] the laser is unconditionally stable for C<1, where factor C is given by:

$$C = (1+\alpha^2)^{1/2} K (\tau_{ext}/\tau_{in}) , \quad (1)$$

and where K is the coupling factor given by [2,3,12,13]:

$$K = \eta_s (1-r_2^2)(r_3/r_2) \quad (2)$$

here, η_s is the mode superposition factor, $r_2^2 \approx 0.35$ for a typical semiconductor surface, while r_3 is target reflectivity.

Regions of unperturbed and unstable dynamics were identified [15] in the r_3-Φ plane, (with $\Phi=2kL$) but without distinguishing between periodic oscillations and chaos, and only for a single value of the α-factor (=3).

From one side, results [12-14] tell us that by an external cavity short with respect to the relaxation-equivalent length, i.e. $L<0.2\ L_{fr}$, and limiting back reflected power to $K^2 < 10^{-7}$ (for $L>L_{fr}$), the regime of oscillations is unconditionally stable. Hence, the rule-of-thumb for a laser used as the source in optical fiber communications is that the return loss from the fiber line should be kept below, say, -70dB, to avoid spoiling the linewidth and increase amplitude noise.

On the other side, in applications we may wish to work at the boundary or well inside the coherence collapse regime. For example, at moderate coupling (1<C<4.6) we take advantage of mode hopping on external cavity modes due to external phase-shift change [1] to realize a self-mixing interferometer.

Another case is when we want to generate chaos or periodic oscillations for applications like chaos cryptography, random number generation and microwave photonics.

Then, we need to explore the regions of coherence collapse in more detail in order to determine preferred areas of operation, e.g., those in which the regime is not very sensitive to parameter variations and can thus be easily controlled. Hence, a study of the regimes generated in the K-τ_{ext} plane is desirable.

In addition, while in a long cavity ($L>L_{fr}$) chaos is only weakly dependent from distance L, in a short-cavity ($L<L_{fr}$) it strongly depends on the phase $\Phi=2kL$. This phase dependence adds another variable, useful to control (or crypt) the generated chaos, making the short-cavity preferable by far.

II. ANALISYS

The DOF system of Fig.1 is modeled by well-known Lang-Kobayashi equations [15] written as:

$$dE/dt = \tfrac{1}{2} [G_N(N- N_0)-1/\tau_p] E + (K/\tau_{in}) E(t-\tau_{ext})\times \times \cos [\omega_0\tau_{ext} +\phi(t)- \phi(t-\tau_{ext})]$$

$$d\phi/dt = \tfrac{1}{2} \alpha\{G_N(N-N_0)-1/\tau_p\} + (K/\tau_{in}) E(t-\tau_{ext})/E(t)\times \times \sin [\omega_0\tau_{ext} +\phi(t)- \phi(t-\tau_{ext})]$$

$$(d/dt)N = J\eta/ed - N/\tau_r - G_N(N- N_0) E^2(t) \quad (3)$$

where (with values used in the calculations):

G_N = modal gain = $8.1\cdot10^{-13}$ m ^{3}s $^{-1}$; K = fraction of field coupled into the oscillating mode (Eq.2); N=carrier concentration (m $^{-3}$); N_0 at inversion =$1.2\cdot10^{24}$ m $^{-3}$; τ_{ext} =2nL/c = round trip time of external cavity; L = distance to external cavity reflector; Φ =2kL external phaseshift; τ_{in} =$2nL_{in}/c$ = round trip time of laser cavity = 5 ps; τ_p = photon lifetime =2 ps; τ_r =carrier lifetime = 2 ns; α = linewidth enhancement factor, (taken 3 - 4.5 - 6); ω_0 = k/c = unperturbed frequency; (λ_0= 1.55 μm); $J\eta$ = pumping current density, and η = internal quantum efficiency; d = active layer thickness; V = active volume= $8\cdot10^{-17}$ m ^{3}.

With the above values, the threshold current was I_{thr}=11 mA, and as in other papers, in all simulations we chose a moderate overdrive factor, J/J_{thr} =1.36 to J=15 mA. The quiescent value of unperturbed electric field E_{00}(for K=0) was found $2.49\cdot10^{10}$.

An important quantity was the relaxation frequency of the unperturbed laser, given by the theoretical expression [3]:

$$f_r = (2\pi)^{-1}[(G_N J_{thr}/ed)(J/J_{thr}-1)]^{1/2} \quad (4)$$

With the numerical values noted above, Eq.4 gives f_r =2.49 GHz. To check consistency with our set of parameters, we looked at the transient of field amplitude E obtained from the L-K equations. Going close to coherence collapse with K, we observed a slowly damped oscillation of E, with a frequency of 2.52 GHz, in reasonable agreement with Eq.4.

Accordingly, the length equivalent $L_{fr}=c/2f_r$ of relaxation frequency is L_{fr}=60 mm for our set of simulation parameters, so from previously published data [13,14] we expect a stable regime for $L<0.1\text{-}0.2\cdot L_{fr}$ = 6-12 mm also at high K values, and nearly total collapse at L>60 mm, where only very small K values can be tolerated.

III. TRANSITION FROM SHORT TO LONG CAVITY

The L-K equations (Eqs.3) have been simulated with the standard Runge-Kutta method for the following range of parameters: distance of external target L = 7.5, 15 and 30 mm (so that L/L_{fr}=0.125, 0.25 and 0.5); coupling factor K = 0.01 to 0.5 in steps of 0.05; linewidth enhancement factor α = 3, 4.5 and 6; phase excess of external target $2kL=\Phi$, taken as $\omega\tau_{ext}/\pi$ from -1 to +1 in steps of 0.05. Typical results are reported in Figs.2 and 3, and are illustrative of periodic and chaos regime, as already described and in agreement with previously published results [3,13,14]. Additionally, a sequence of time series and spectra obtained from the L-K equation for L= 7.5mm, K=0.5, and α=6, as the phase Φ varies from -π to +π is provided in a movie [16]. This sample is illustrative also of other cases, and tells us how the regimes are easily classified by direct inspection of the amplitude and spectra panel.

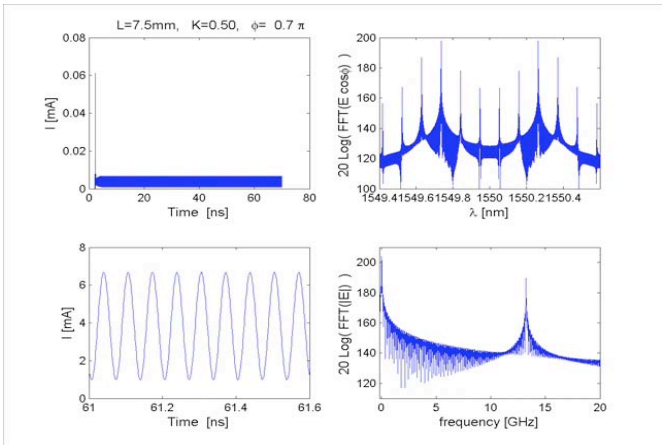

Fig.2. Multiperiodic oscillations of DOF at L= 7.5, α=6, K=0.5, and $\omega_0\tau_{ext}/\pi$=0.7. From top left counterclockwise: current I=$<|E^2|>$ on a slow scale, current I on a fast time scale (zoomed after 30ns), electrical spectrum of current I and spectrum of optical signal E cos(ωt+ϕ) reported at the central wavelength λ=1550 nm.

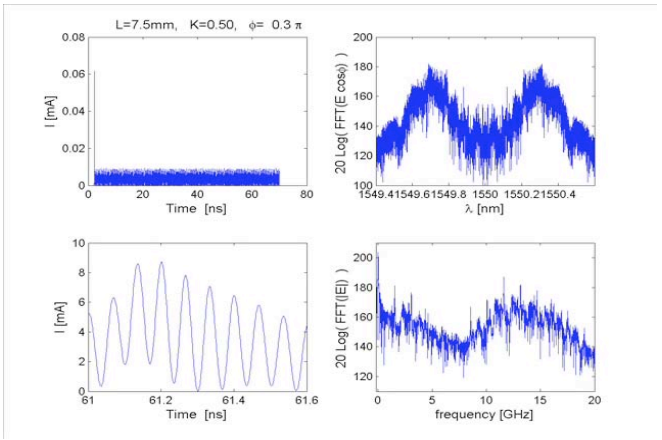

Fig.3. Chaos oscillations of DOF at L= 7.5, α=6, K=0.5, and $\omega_0\tau_{ext}/\pi$=0.3. As in Fig.2, from top left counterclockwise we display: current on slow and fast time scale, electrical spectrum of current and spectrum of optical signal.

Figs. 4 and 5 summarize the regime evolution at decreasing lengths of the external reflector, i.e. with L=30, 15, 7.5 and 3,75 mm. The plane Φ-K is colored according to the regime of oscillation, classified by inspection of their panels, as shown in Figs. 2-3, in chaos, multiperiodic, single-periodic, and unperturbed/self-mixing. For all the lengths, diagrams are presented for three values of α, namely 3, 4.5, and 6.

As we can see from Fig.4, increasing the alpha factor makes the regime more complex (or chaotic), as because the diagrams are half-filled with chaos for α=3, have just a few residual multiperiodic stripes for α=4.5, and become chaotic almost everywhere (except for K<0.01) for α=6. In the last case, the dependence on phase Φ is practically lost.

Decreasing the length from L=30 to 15, 7.5 and to 3.75 mm causes the high-level dynamics behavior to become more confined, and chaos stripes narrower (Fig.5). For example, as α decreases from 6 to 3, at L=15mm, the stripes become more widely spaced apart, while wide unperturbed (or self-mixing) regions open up and increase at low K values.

It is interesting to note, that, for L=7.5mm and α=3 (Fig.7 middle) too, we have chaos stripes starting at K=0.4, though in

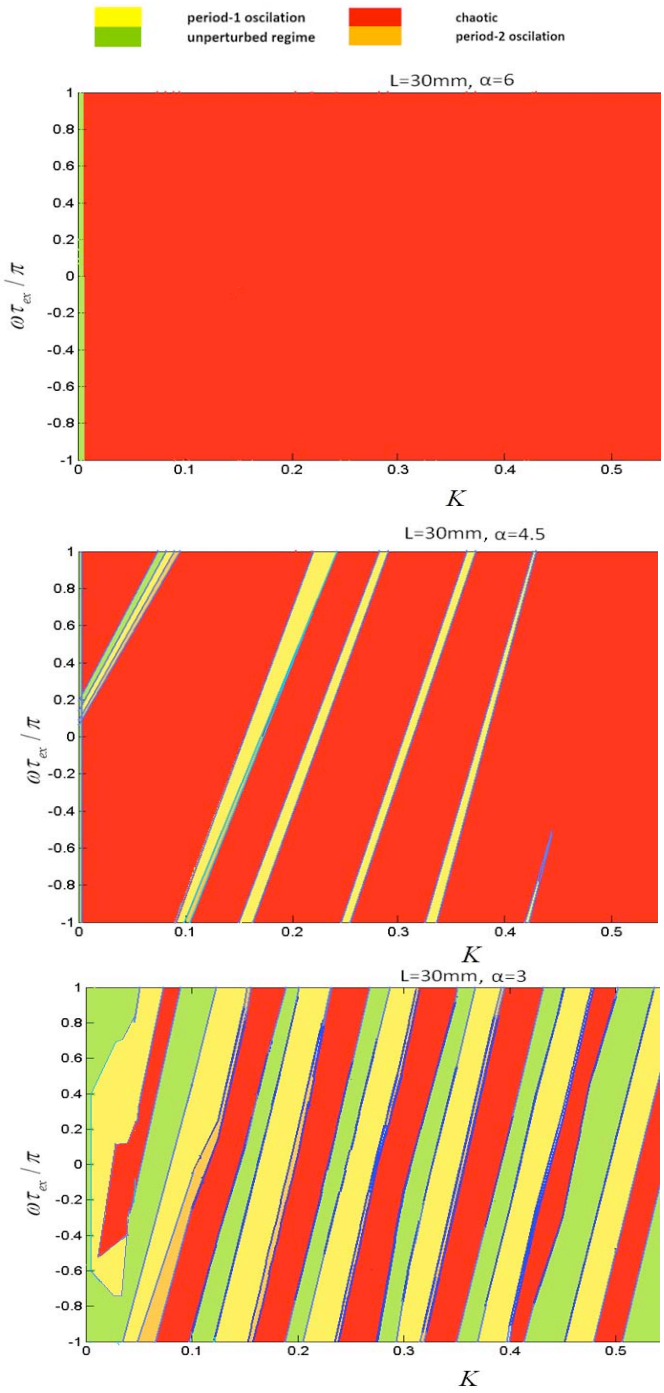

Fig.4. Regimes of DOF system in the plane of phase $\Phi=2kL=\omega_0\tau_{ext}$ and coupling K, for L=30mm, and (top to bottom) α=6, 4.5, and 3. Regimes are indicated by colors: red for chaos, orange multiperiodic, yellow periodic, green unperturbed (or self-mixing). Top diagram, α=6, shows that the system is chaotic for all combinations of K and Φ, except for a narrow interval (green band) close to zero, at K<0.01 (or C<1). The effect of decreasing α is to open the diagram to multiperiodic bands (α=4.5) and for α=3 to stripes of period-1 and unperturbed (or self-mixing) regime.

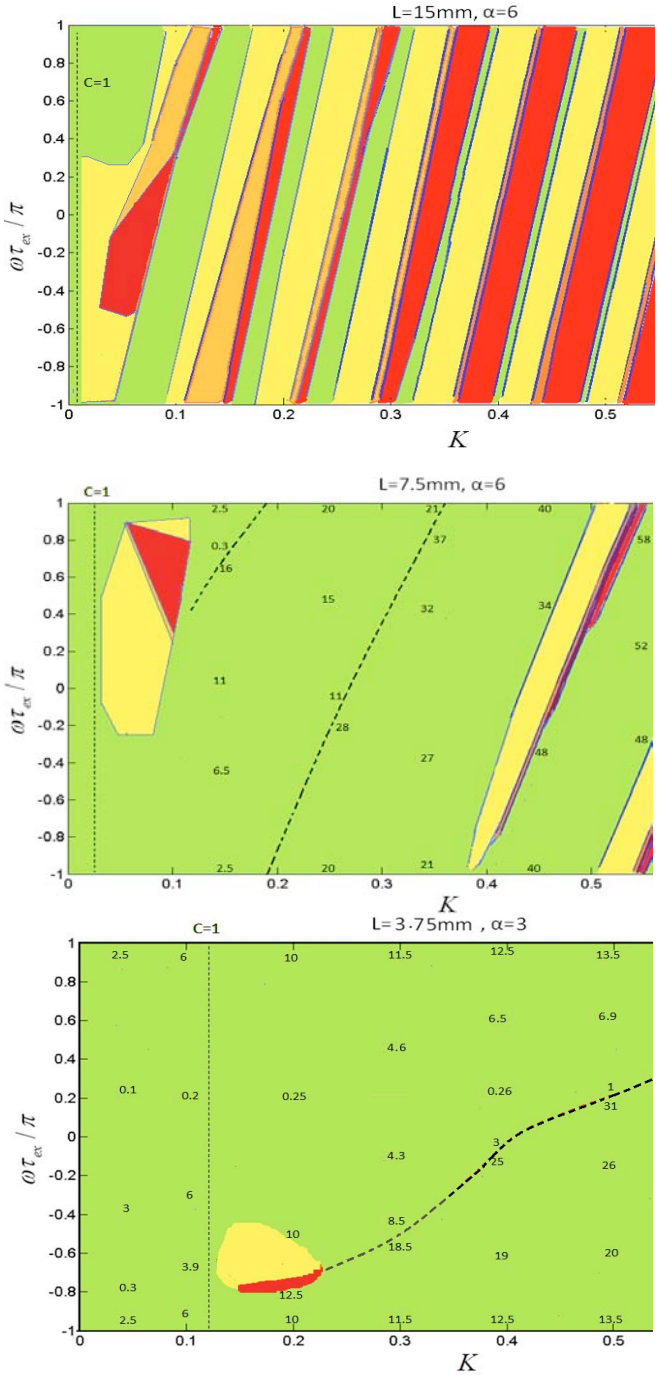

Fig.5. Regimes of the DOF system in the plane of phase $\Phi=2kL=\omega_0\tau_{ext}$ and coupling K, for different target distances at constant $\alpha=3$. From top to bottom: L=15-mm, 7,5-mm, 3.75-mm, Regimes are indicated by colors as above. Stripes of multiperiodicity and chaos become thinner and then disappear as L is decreased. At 3.75-mm, there is a residual island at K≈0.15, isolated in a sea of unperturbed (or self-mixing) oscillation regime. Numbers give the self-mixing induced Δν in GHz. The dotted curve is the location of frequency switching of the Δν. The thin vertical line is the limit C=1.

a thin ΔK≈0.1 interval. This length L=7.5mm corresponds to $L/L_{fr}=0.125$, a value usually considered to belong to the stable regime of oscillations.

When L=3.75 mm (Fig.5 bottom), the Φ-K plane is almost completely filled with green, i.e., an unperturbed/self-mixing regime. However, also at the small ratio $L/L_{fr}=0.0625$ we find a residual small island, at K ≈0.14-0.21 and $\Phi/\pi=0.5$-0.7, of chaos regime, similar to the one already seen for L=7.5mm, $\alpha=3$ and K≈0.1, surrounded by an unperturbed regime.

The existence of this island is surprising, and we double-checked the calculations to verify its presence. Actually, the island was also noticed by Jones et al. [16], but up to now the reason for its existence is not fully understood.

Interestingly, the left edge of the islands is tangent to the C=1 line (dotted line in Fig.5), consistent with the fact that at C<1, the regime is unconditionally stable and strictly single mode (with no switching on ECM - external cavity modes).

IV. The Feedback Diagram Revisited

The diagram of feedback effects, also called Tkach and Chraplyvy (T-C) diagram [17] has been the reference for classifying feedback effects in semiconductor laser subjected to retro-reflections from a remote target [18]. The T-C diagram identifies five regimes of feedback (see Fig.6), and since its publication has become the milestone reference cited in literature and reported in textbooks [19].

At the time the T-C diagram was developed, feedback was regarded mainly as a disturbance affecting the performance of linewidth and amplitude noise of a laser, and impairing the use of the source in optical fiber communication systems.

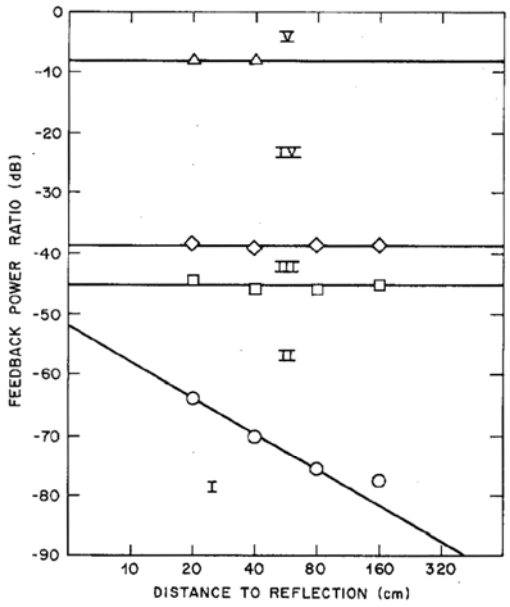

Fig.6. The original T-C diagram of back-reflection attenuation (in dB) versus external cavity length L. According to the original description, region I correspond to linewidth narrowing/broadening (depending on the phase of feedback), II to line splitting and mode-hopping, III return to single-mode narrow-line operation, IV to coherence collapse, V to oscillation on the external cavity. As feedback ratio is expressed in dB, numbers on Y-axis apply both to power attenuation and to electric field amplitude attenuation K. (From [17], by courtesy of the IEEE).

The picture presented by T-C diagram to the user of laser diode as a source for fiber optics communications warned that only very weak returns (possibly down to < -80 dB) can be tolerated with no penalty on noise and linewidth of the source.

In the years to follow, however, high-level dynamic effects in laser diodes have been studied in much more detail, and the evolution and descriptive character of the oscillation, characterized by field amplitude E and phase ϕ, not linewidth only. Also pointed out, and confirmed by Sections II and III of this paper, we need consider additional parameters affecting the dynamics to fully account for the laser behavior, namely: (i) the optical phase associated to distance, 2kL (mod 2π) when $L<c/2f_2$ (the case of *short* cavity); (ii) the distance L being smaller or larger than the coherence length L_{coh} of the unperturbed source, i.e., the cases of *coherent* and *incoherent* feedback; and (iii) of course, all the constitutive parameters (gain, loss, photon and carrier lifetimes, etc.) with especially the alpha factor to influence the dynamical regime behavior.

Rather than undesired disturbance to be avoided, the weak feedback regime (region I), started to attract interest in 1990's in measurements: feedback affects the oscillating field both in amplitude and frequency and AM and FM modulations carry signals ΔE and $\Delta\nu$ related to and useful for the measurement of amplitude and phase of the returning field [1].

In conclusion, going back to the T-C diagram, we can redraw the bottom part of it as in Fig.7, showing that in region I and II we encounter the self-mixing regime of AM and FM modulations, with sine/cosine wave dependence on external optical path-length at weak feedback and small C, and with distorted sinusoid waveforms at increased C, up to the switching promoted by hopping on external mode resonances.

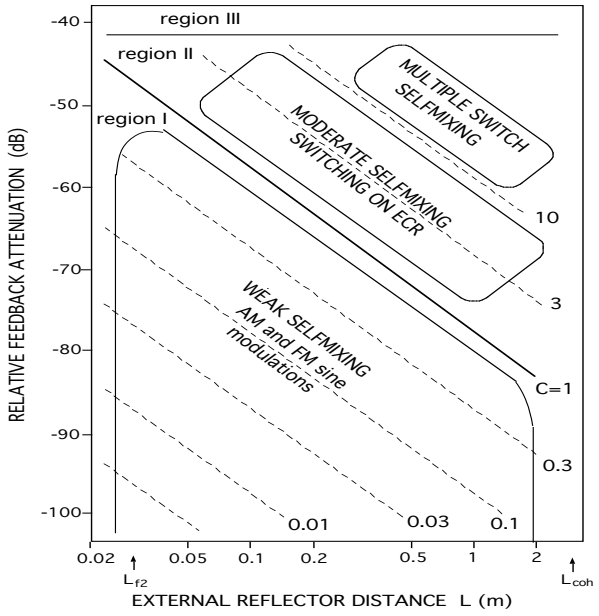

Fig.7 Revisiting the bottom part of the T-C diagram, across regions I, II and III: at weak feedback we find the regime of self-mixing, with AM and FM modulations of the cavity field driven by the external path-length phase 2kL. Increasing the feedback at C=1 and larger, we find the moderate feedback regime with switching on external cavity resonance (ECR), initially single (one per period), then multiple for C>10.

From the point of view of applications developed in these regions, we find, as depicted in Fig.8, the 2- channel SMI and the injection detection up to about C≈0.1, then the moderate feedback, 1-channel SMI starting at C>1 and up to C≈10 with proper signal processing. The self-mixing coherent injection detection (SMD) and the SMI share a common noise floor limitation, at typically -90 dB [1], due to the quantum noise associated with the detected photons [1,18, 20, 21].

At the opposite end of high level of signals, we may find a limit due to saturation of the field amplitude and switching of signal waveform, at C≈1, at about -40...-30 dB. Last, in Fig.7 we also draw the limit of maximum distance L of the external reflector, as due to decreased signal amplitude and limit of coherence length L_{coh}, a few meters on assuming a linewidth of some tens of MHz.

On increasing the K factor over a certain threshold, the system is driven into a *strong interaction* characterized by the generation of sidebands that gradually increase in amplitude and number (periodicity and multiperiodicity regimes) until they fill-up all the phase space, as seen in Fig.4.

First question to be considered is the boundary of *weak* versus *strong* interaction regimes. Different criteria have been proposed [12-15] like linewidth analysis, stability of the L-K equations and Lyapunov's exponent. Findings differ somehow, yet they allow some general conclusions on the "unperturbed" regime, by means of three regions in the T-C diagram, as follows.

At large feedback (K up to $\approx 10^{-2}$) it should be $f_2\tau_{ext}<0.1$-0.2 (or, $L<0.1$-0.2 L_{f2}); at intermediate strength of feedback we shall stay at C<1; and at weak feedback (and $L>L_{f2}$) we should keep $K<\approx 2\cdot 10^{-4}$ (or -74 dB). The asymptotes corresponding to these conditions are plotted in Fig.8 as dotted lines (the last after a scale break). Actually, as discussed in Section II and III the unperturbed condition is never reached, because the self-mixing regime is found everywhere in the K-L diagram. We can say that retro-reflection leaves the laser source "unperturbed" only by reference to a specific condition, like e.g., limited linewidth broadening as assumed in early works [12-15]. Indeed, when the self-mixing FM modulation term sin 2kL is small and concealed in the natural frequency line, we can take the source as "unperturbed" from the engineering point of view. This happens when the frequency deviation by the self-mixing is less than say, $\Delta\nu\approx 10$ MHz. Also in this case, unnoticed in early work, a small amplitude dependence from cos 2kL still remains, however of the order of -60 to -40 dB (for K=-40dB or less). The level is small enough to be negligible if the laser is used as a transmitter in communications, while it is well revealed and useable in an interferometer and for echo detection [1,18,21].

At higher K, the frequency deviation $\Delta\nu$ rapidly increases up to GHz's and tens-of-GHz range, always and only as a self-mixing AM and FM effect excluding any randomness in E and ϕ, and multiperiodicity and chaos effects.

Thus, we suggest a new nomenclature to distinguish the two cases: *weak self-mixing regime* (for the quasi-unperturbed state), and *strong self-mixing regime* for sizable AM and FM

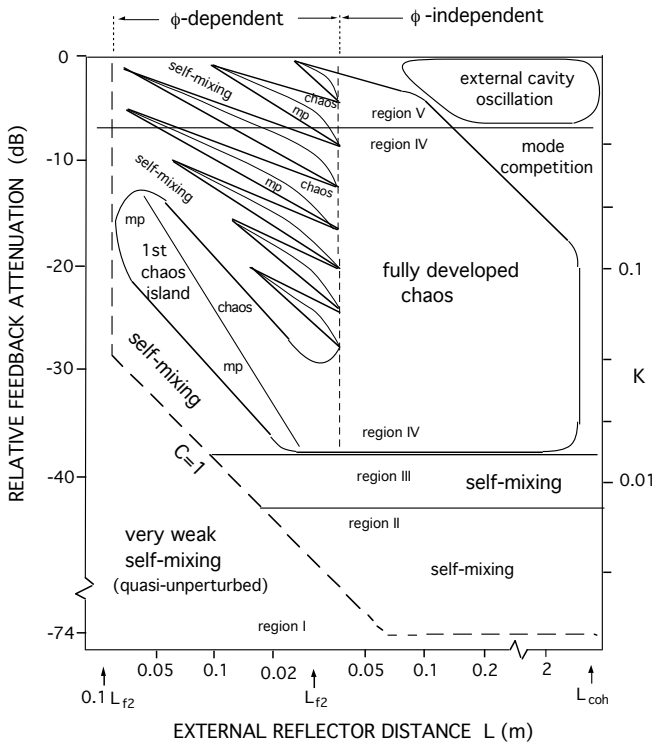

Fig.8 The T-C diagram revisited, across regimes III, IV and V. Dotted lines are the boundary of "unperturbed" operation, (or self-mix only), with unnoticeable linewidth broadening. The asymptote at -74dB is included in the diagram after a Y-scale break. Another scale break, on X-axis, is used to accommodate L_{coh}. Increasing K and at small L, beyond region III we find an island of chaos and multiperiodicity. At these short ($L<L_{f2}$) external cavity, the regime is dependent on optical phase $\phi=2kL$ and it changes from unperturbed to period-1, to multiperiodic, and chaos, with just a small variation of ϕ. The diagonal thin line in the island gives the relative proportion of chaos and multiperiodicity (mp). On the left side, the island is almost tangent to the unperturbed vertical asymptote (dotted line), and on the right side merges with the fully developed chaos at a length $L\approx L_{f2}$. All around the island there is a sea of self-mixing regime, this time with sideband frequency in the GHz and up to several 10-GHz range. Above the island we find triangular stripes of multiperiodicity and chaos, ϕ-dependent, which increase in width as L increases and finally merge to the right into the chaos area (thin dotted line). At still higher L, starting from about L_{f2}, we enter a broad area of long-cavity, phase-independent and fully developed chaos. Above about -5 dB chaos ceases because the system oscillates on the external cavity. Starting from distances of the order of the unperturbed coherence length ($L\geq L_{coh}$) the system exhibits self-locking and unlocking in frequency due to the reflected waves, and bistability.

sideband generations. These add to the well-known cases of *periodicity, multiperiodicity* and *chaos*.

Now, considering the upper part of the T-C diagram (Fig.8), let's go across regions III, IV and V. At the left side of the diagram, when the external cavity length is small ($L\approx 0.1L_{f2}$), on increasing K of about 10-dB with respect to the C=1 boundary, we encounter a first island of chaos and multi-periodicity, as described in Sect.II and III.

Of course, we cannot represent the phase-dependent evolution in the T-C diagram of Fig.8, but in Ref.[22] the reader can find the full sequence of waveforms on a phase cycle for several combinations of parameters K, L, α.

As we move to increased length L, the corresponding K decreases (of about 20-dB/decade) down to about -40 dB, the boundary of T-C region III.

Meanwhile, the relative occurrence in a 2π Φ-cycle of chaos and multiperiodicity is changed, with the chaos proportion increasing steadily up to fill all the available phases. This is rendered by the thin line running in diagonal in the island. When we reach $L=L_{f2}$ in the island of Fig.8, the regime is only chaotic, and becomes phase-independent, a well-known feature of long external cavity.

Going above the island, we first return to self-mixing regime for a certain range of K values, then, we encounter a number of triangular stripes. These are regions of chaos and multiperiodicity depending on phase Φ, in addition to K and L. The stripe width is constant across the K-Φ plane, while it increases almost linearly with L and α. Thus, in the K-L diagram of Fig.8, the stripes are triangle-shaped and placed along a diagonal. They encompass chaos and multiperiodic oscillation, and are separated by strong-self-mixing regime, with frequency of sideband ranging from several GHz up to several 10-GHz. Inside the stripes, we find again a proportion of Φ--dependent chaos and multiperiodicity, increasing from left to right (as indicated by the thin line inside the stripes) and becoming all-chaos as we approach the base of the stripes, at $L=L_{f2}$. Here, the chaos becomes phase-insensitive and we only get chaos in an uninterrupted wide range of K and L.

Till now, we have tacitly assumed a condition of coherent superposition for the returned field. However, also the case of incoherent feedback interaction is interesting.

An incoherent return actually affects the mode oscillating in a semiconductor laser, because the square-field term E^2 in the last L-K equations (Eq.3) depletes the state density N.

Incoherent superposition is found when the return is from a distance $L>L_{coh}$, or when the re-injected mode is orthogonal to a pre-existing, in-cavity mode. One way to obtain an orthogonal mode is rotating the state of polarization of returning field by 90-deg. Ju and Spencer [23] have studied polarization-rotated feedback, which obviously is independent from distance L and phase Φ. At levels of K high enough, they found regime of chaos, self-pulsation, and two-state oscillation. Clearly, no self-mixing regime can be found in incoherent feedback, and at very low K the source is now really unperturbed.

Turning now to applications of high-level dynamics, probably the most actively pursued in recent years, internationally, has been chaos cryptography.

So, the T-C diagram is the adequate means to represent the area of operation of DOF-based systems for cryptography.

A fully developed chaos is found the best for a good synchronization, and thus L will span from L_{f2} (=30 mm from Fig.8, eventually up to 100 mm, adjustable with the laser bias current), to perhaps a maximum of 3-5 times as much. Considering a $n_{in}=3.5$ as the effective index of refraction of the waveguide semiconductor material, we will take the guide length L_g in the range L_g =10 to 50 mm.

About the K factor, in the IPC we may use either a cleaved facet for the reflector ($r_3 \approx 0.55$) or have the end-face multilayer coated for maximum reflectance and hereafter add an absorber section along the path for the user to trim reflectance. So, the K factor can range from 0.3 to 0.8 in practice.

Other applications of high-dynamic DOF systems are related to microwave tone generation [24], utilizing the period-1 regime; this was the original proposal based on an injection coupling laser (ICL) scheme. The frequency range covered can span from a few GHz up to several times the modulation cutoff frequency f_2.

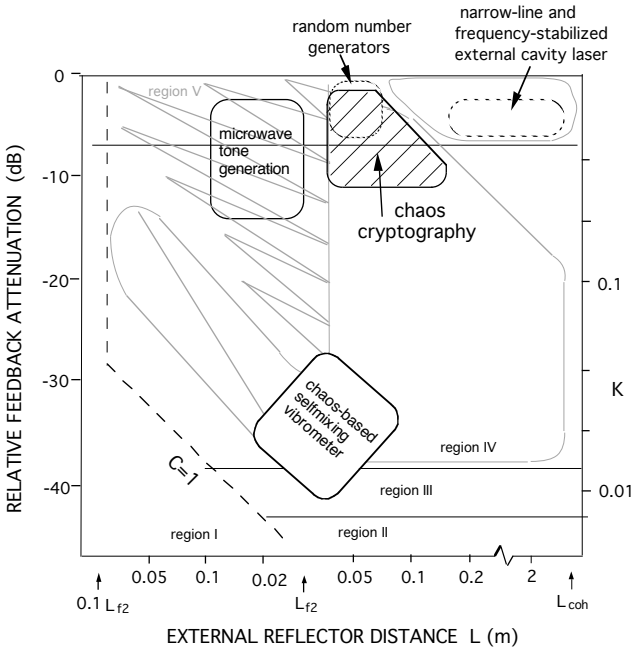

Fig.9 Preferred areas of operation for some applications using the regimes of Fig.8: chaos cryptography by DOF (dashed area) random number generation (thin-dot line), microwave tone generation, chaos-based SMI vibrometry, and external cavity frequency stabilized laser.

Further, some applications of chaos to instrumentation have been reported. One is the extension to very high C regime of the basic self-mixing principle (see Fig.9), by which a demodulated waveform $\Phi=2kL$ is obtained in place of the normally expected sin Φ. Another proposal [24] is to use chaos to remove the range ambiguity of a conventional sine-wave modulated telemeter, checking the maximum of the autocorrelation function to determine distance; for this feature the best area of operation is again that of the random number generation.

Last, an application indicated in Fig.9 is related to chaos suppression, that of oscillation on the external cavity to possibly develop a narrow-line, frequency-tunable laser. A variant of the well-known external-cavity scheme, the design usually starts with a reduced-reflectivity r_2 (or an ARC output facet) and a grating as the external target. A three-mirror approach allows us to take account of the non-vanishing reflectivity r_2, and use uncoated chip as the source.

REFERENCES

[1] S. Donati: "Developing Self-Mixing Interferometry for Instrumentation and Measurements" *Laser Photonics Review*, vol.6 (2012), (DOI) 10.1002/lpor.201100002.

[2] D.M. Kane, K.A. Shore: "Unlocking Dynamic Diversity- Optical Feedback effects on Semiconductor Lasers", J.Wiley & Sons, London, 2008.

[3] K. Ohtsubo: "Semiconductor Lasers: Stability, Instability and Chaos". Springer Series Optical Sciences vol.111, New York, 2006.

[4] S. Donati, C.Mirasso: (Editors): "Optical Chaotic Cryptography", Feature Issue of: *IEEE Journal of Quantum Electronics*, vol. QE-38, pp.1138-84.

[5] A.Argyris, D.Syvridis, L.Larger, V.Annovazzi, P.Colet, I.Fischer, J.Garcia-Ojalvo, C.Mirasso, L.Pasquera, K.A.Shore: "Chaos-based Communication Link at high bit rate using Commercial Fiber Optic Link" *Nature Letters,* Nov.2005, pp.343-346.

[6] V. Z. Tronciu, C. Mirasso, P. Colet, M. Hamacher, M. Benedetti, V. Vercesi, V. Annovazzi Lodi: "Chaos Generation and Synchronization Using an Integrated Source with an Air Gap", *IEEE J. of Quant. Electr.,* vol.46, Dec.2010, pp.1840-1846, see also:

[7] S.Sunada, T.Harayama, K.Arai, K.Yoshimura, P.Davis, K.Tsuzuki, A. Uchida, "Chaos Laser Chip with Delayed Optical Feedback using a Passive Ring Waveguide", *Optics Express*, vol.19, 2011, pp.5713-5724.

[8] A.Argyris, S.Deligiannidis, E.Pikasis, A.Bogris, D.Syvridis: "Implementation of 140 Gb/s True Random bit Generator Based on a Chaotic Photonic Integrated Circuit", *Optics Express*, vol.18 (2010), pp.18763-168

[9] K.Myneni, T.A.Bar, B.R. Reed, S.D.Petel, N.J.Corron: "High-Precision Ranging Using a Chaotic Pulse Train" *Appl. Phys. Lett.* vol.78, 2001, pp.1496-1499, see also: F.Y.Lin, J.M. Liu: " Chaotic Lidar", *IEEE Journal of Secl. Topics in Quantum Electro.,* vol.10, 2004, pp.991-997.

[10] S.K. Hwang, S.C. Chan, S.C. Hsieh, and C.Y. Li, "Photonic microwave generation and transmission using direct modulation of stably injection-locked semiconductor lasers," *Opt. Commun.* vol.284, pp.3581–89. 2011.

[11]S. C. Chan, S.K.Hwang, J.M. Liu: "Radio-over-Fiber AM-to-FM- Upconversion Using an Optically Injected Semiconductor Laser", *Opt. Letters*, vol.31, 2006, pp.2254-2256.

[12] P.Spencer, P.Pees, I.Pierce:"Theoretical Analysis", Chapter 2 of Ref. 2.

[13] J.Mork, B.Tromberg, J.Mark: "Chaos in Semiconductor Lasers with Optical Feedback: Theory and Experiments", *IEEE Journal Quant. Electr.,* vol.28, 1992, pp.93-108.

[14] R.J. Jones, P.S. Spencer, J.Lawrence, D.M.Kane: "Influence of the External Cavity Length on the Coherence Collapse Regime in Laser Diodes Subject to Optical Feedback", *IEE Proc. part J, Optoelectronics*, vol.148 (2001), pp.7-12.

[15] R. Lang and K. Kobayashi, "External Optical Feedback Effects on Semiconductor Injection Laser Properties", *IEEE J. Quant. Electr*., vol.QE-16 (1980), pp.347-355. see also: R. Ju, P.Spencer: "Dynamic Regimes in Semiconductor Lasers Subjected to Incoherent Optical Feedback", *IEEE J. Lightwave Technol*., LT-23 (2005), pp.2513-2523.

[16] see http://www-3.unipv.it/donati/Movie1alfa6.wmv

[17] R. W. Tkach and A. R. Chraplyvy: "Regimes of Feedback Effects in 1.5-um Distributed Feedback Laser" *IEEE J. Lightwave Technol.*, LT-4, (1986), pp. 1655-1661.

[18] S. Donati: "*Photodetectors*", Prentice Hall, Upper Saddle River, N.J., 2000, see Sect.8.4.

[19] K. Petermann: "*Laser Diode Modulation and Noise*", Kluwer Academic Publ., Dodrecht, 1991.

[20] S. Donati: "*Electro-Optical Instrumentation*", Prentice Hall, Upper Saddle River, N.J., 2004, Sect.4.5.2.

[21] S. Donati: "Responsivity and Noise of Self-Mixing Photodetection Schemes", *IEEE Journal Quantum Electronics*, vol. QE-47, 2011, pp.1428-1433.

[22] S. Donati, M.T.Fathi: "Transition from Short-to-Long Cavity and from Self-Mixing to Chaos in a Delayed Optical Feedback Laser", *IEEE Journal Quantum El*. vol.QE-48, 2012 , pp.1352-1359.

[23] R. Ju, P.S. Spencer: "Dynamic Regimes in Semiconductor Lasers Subjected to Incoherent Optical Feedback", *IEEE J. Lightwave Technol.,* LT-23 (2005), pp.2513-2523

[24] S.Donati, S.-K. Hwang: "Chaos and High-Level Dynamics in Coupled Lasers and their Applications", *Progress in Quantum Electronics*, vol.36, Issues 2–3, March–May 2012, pp. 293–341.